



Identification of the susceptibility genes for COVID-19 in lung adenocarcinoma with global data and biological computation methods



Li Gao^a, Guo-Sheng Li^a, Jian-Di Li^a, Juan He^a, Yu Zhang^b, Hua-Fu Zhou^c, Jin-Liang Kong^d, Gang Chen^{a,*}

^a Department of Pathology, The First Affiliated Hospital of Guangxi Medical University, No. 6 Shuangyong Rd, Nanning, Guangxi Zhuang Autonomous Region 530021, PR China

^b Department of Pathology, Shandong Provincial Hospital Affiliated to Shandong First Medical University, No. 324. Jingwu Rd, Jinan, Shandong 250021, PR China

^c Department of Cardio-Thoracic Surgery, The First Affiliated Hospital of Guangxi Medical University, No. 6 Shuangyong Rd, Nanning, Guangxi Zhuang Autonomous Region 530021, PR China

^d Ward of Pulmonary and Critical Care Medicine, Department of Respiratory Medicine, The First Affiliated Hospital of Guangxi Medical University, No. 6 Shuangyong Rd, Nanning, Guangxi Zhuang Autonomous Region 530021, PR China

ARTICLE INFO

Article history:

Received 6 August 2021

Received in revised form 7 November 2021

Accepted 16 November 2021

Available online 20 November 2021

Keywords:

LUAD

COVID-19

DEG

Susceptibility

Immune infiltration

WGCNA

ABSTRACT

Introduction: The risk of infection with COVID-19 is high in lung adenocarcinoma (LUAD) patients, and there is a dearth of studies on the molecular mechanism underlying the high susceptibility of LUAD patients to COVID-19 from the perspective of the global differential expression landscape.

Objectives: To fill the research void on the molecular mechanism underlying the high susceptibility of LUAD patients to COVID-19 from the perspective of the global differential expression landscape.

Methods: Herein, we identified genes, specifically the differentially expressed genes (DEGs), correlated with the susceptibility of LUAD patients to COVID-19. These were obtained by calculating standard mean deviation (SMD) values for 49 SARS-CoV-2-infected LUAD samples and 24 non-affected LUAD samples, as well as 3931 LUAD samples and 3027 non-cancer lung samples from 40 pooled RNA-seq and microarray datasets. Hub susceptibility genes significantly related to COVID-19 were further selected by weighted gene co-expression network analysis. Then, the hub genes were further analyzed via an examination of their clinical significance in multiple datasets, a correlation analysis of the immune cell infiltration level, and their interactions with the interactome sets of the A549 cell line.

Results: A total of 257 susceptibility genes were identified, and these genes were associated with RNA splicing, mitochondrial functions, and proteasomes. Ten genes, MEA1, MRPL24, PPIH, EBNA1BP2, MRT04, RABEPK, TRMT112, PFDN2, PFDN6, and NDUFS3, were confirmed to be the hub susceptibility genes for COVID-19 in LUAD patients, and the hub susceptibility genes were significantly correlated with the infiltration of multiple immune cells.

Conclusion: In conclusion, the susceptibility genes for COVID-19 in LUAD patients discovered in this study may increase our understanding of the high risk of COVID-19 in LUAD patients.

© 2021 The Author(s). Published by Elsevier B.V. on behalf of Research Network of Computational and Structural Biotechnology. This is an open access article under the CC BY-NC-ND license (<http://creativecommons.org/licenses/by-nc-nd/4.0/>).

Abbreviations: LUAD, lung adenocarcinoma; DEG, differentially expressed genes; SMD, standard mean difference; COVID-19, coronavirus disease 2019; SARS-CoV-2, severe acute respiratory syndrome coronavirus 2; WGCNA, weighted gene co-expression network analysis; FPKM, fragments per kilobase per million; TPM, transcripts per million reads; GTEX, Genotype-tissue Expression; FC, fold change; CI, confidence interval; PPI, protein-to-protein interaction; SROC, summarized receiver's operating characteristics; IHC, immunohistochemistry; HPA, human protein atlas; TF, transcription factor.

* Corresponding author.

E-mail address: chen_gang_triones@163.com (G. Chen).

<https://doi.org/10.1016/j.csbj.2021.11.026>

2001-0370/© 2021 The Author(s). Published by Elsevier B.V. on behalf of Research Network of Computational and Structural Biotechnology.

This is an open access article under the CC BY-NC-ND license (<http://creativecommons.org/licenses/by-nc-nd/4.0/>).

1. Introduction

Coronavirus disease 2019 (COVID-19) has swept across the globe since it was first identified in December 2019 in Wuhan, China, and severe acute respiratory syndrome coronavirus 2 (SARS-CoV-2) is the primary culprit behind COVID-19 [1,2]. To date, COVID-19 has resulted in over 72 million diagnosed cases and more than 1 million deaths, posing a serious threat to the public [3]. Factors such as age and comorbidities may affect the severity of clinical manifestations of COVID-19, which include mild or no pneumonia, fever, headaches, hemoptysis, myalgia, fatigue, and sputum production [4,5]. The pervasion of the virus is attributed

to the transmission route from person to person via saliva droplets, direct contact with COVID-19 patients, or aerosol transmission [2,6]. Although the public is susceptible to COVID-19, elderly people and people with health conditions, such as cardiovascular disease, chronic obstructive pulmonary disease, hypertension, cancer, and diabetes mellitus, are more predisposed to the more severe symptoms of COVID-19 [7–9]. A recent cohort study by Liang et al. pointed out the higher incidence of cancer in COVID-19 patients than in normal populations and the fact that COVID-19 patients with cancer were also more likely to suffer from acute complications than those without cancer [10]. Lung cancer has been found to be the most common type of cancer in COVID-19 patients [11]. Considering the association between lung cancer and COVID-19 and the highest frequency of lung adenocarcinoma (LUAD) among all histological subtypes of lung cancer, it is necessary to dig into the molecular mechanism underlying the high susceptibility of LUAD patients to COVID-19.

Despite the fact that the molecular basis for the susceptibility of LUAD patients to COVID-19 has been investigated by several studies, these studies all focused on the ACE2 SAR2-Cov-2 receptor [12–14]. The crucial importance of ACE2 in the high vulnerability of LUAD patients to COVID-19 needs not be emphasized. Apart from ACE2, numerous other genes and pathways may play essential roles in the susceptibility of LUAD patients to COVID-19, and these factors have not been extensively investigated by prior studies. To fill this research void, the present work identifies genes correlated with the susceptibility of LUAD patients to COVID-19 via biological computational methods and by calculating standard mean difference (SMD) values for differentially expressed genes (DEGs) in 49 SARS-CoV-2-infected LUAD samples and 24 non-affected LUAD samples, as well as 3931 LUAD samples and 3027 non-cancer lung samples from the 40 most pooled RNA-seq and microarray datasets, which created the most complete LUAD dataset assembled so far. The susceptibility genes for COVID-19 in LUAD were annotated with their biological functions, and hub susceptibility genes significantly related to COVID-19 were selected via a weighted gene co-expression network analysis (WGCNA). Then, the hub genes were further analyzed via the examination of their clinical significance in multiple datasets, a correlation analysis with immune cell infiltration levels, and their interactions with the interactome sets of the A549 cell line. The present study is anticipated to stimulate strategies that can be used to help LUAD patients with COVID-19.

2. Materials and methods

2.1. Accumulation of global RNA-seq and microarray datasets for LUAD

We searched the TCGA and Genotype-tissue Expression (GTEx) databases to obtain level-three fragments per kilobase per million (FPKM) and transcripts per million reads (TPM) of RNA-seq data of 533 LUAD and 347 normal lung samples (288 normal cases and 533 tumor cases from the TCGA database; 59 normal cases from the GTEx database). The FPKM expression matrix was converted to a TPM expression matrix and normalized with the $\log_2(x + 0.001)$ algorithm.

Other databases, including GEO, ArrayExpress, SRA, and OncoPrint, were searched for microarrays containing gene expression data for LUAD and non-cancer lung samples. The following search strategies were used to retrieve the microarrays: “cancer OR carcinoma OR tumour OR tumor OR malignan* OR neoplas*” AND “Lung OR pulmonary OR respiratory OR respiration OR aspiration OR bronchi OR bronchioles OR alveoli OR pneumocytes.” The details of each RNA-seq and microarray dataset, including accession ID,

country, platform, sample type, and sample numbers, were extracted and compiled together. The processing of all included microarrays followed the steps of probe matching, \log_2 transformation if possible, averaging for repeated items, and normalization between arrays. If several GSE datasets were generated from the same GPL platform, they were merged into one dataset, and the batch effect was removed from these datasets with the *sva* and *limma* packages of R software v.3.6.1.

2.2. The DEGs of LUAD identified from all collected datasets

The index of (SMD) was used to summarize continuous variables with different units of measurement and large differences in mean. We successfully applied the methods of calculating SMD values to the gathered datasets to comprehensively evaluate the expression trends of specific genes in human cancers. In the present work, differential expression analysis for all RNA-seq and microarrays was performed with the *limma* package of R software V.3.6.1. Genes with significant aberrant expression in LUAD samples of any of the included datasets according to differential expression analysis (\log_2 fold change (FC) value of >1 or <-1 and adjusted P value < 0.05) were reserved for further estimation of SMD values. The SMD values with 95% confidence intervals (CIs) were computed based on data including the number of samples, mean, and standard deviation of expression values in the LUAD and non-cancer groups. A meta package of R software v.3.6.1 was utilized for the calculation of SMD values for all reserved genes. Up-regulated reserved genes ($\log_2FC > 1$, adj. P < 0.05) with SMD values and 95 %CI > 0 were defined as upregulated DEGs in LUAD, and down-regulated reserved genes ($\log_2FC < -1$, adj. P < 0.05) with SMD values and 95 %CI < 0 were defined as down-regulated DEGs in LUAD.

2.3. The susceptibility genes for COVID-19 in LUAD

In the current study, two microarrays from the GEO database, GSE147507 and GSE163547, were included to obtain the DEGs between SARS-CoV-2-infected LUAD samples and non-affected LUAD samples [15,16]. The *limma* package for R software has been widely used in differential expression analyses of microarrays as well as RNA-seq data. It was crucial to normalize the expression values of all the samples before making meaningful comparisons between different groups of samples on the same measurement scale [17]. Therefore, the R package known as *biomaRt* was first used to infer the transcript per million (TPM) expression matrix from the original count expression matrix of GSE147507. Following the normalization of the expression matrix, differential expression analysis was applied to the two microarrays. The screening criteria for DEGs were \log_2FC values of >1 or <-1 and adjusted P values < 0.05 . The intersection of up-regulated DEGs in LUAD (part 2.2) and up-regulated DEGs in SARS-CoV-2-infected LUAD samples was designated as the susceptibility gene for COVID-19 in LUAD patients.

To understand the enrichment of susceptibility genes in terms of biological processes, cellular components, molecular functions, and KEGG pathways, we performed functional annotations of these susceptibility genes using the *ClusterProfiler* R package after the determination of susceptibility genes for COVID-19 in LUAD patients. P < 0.05 indicated significant functional annotation. The interrelationships between susceptibility genes and biological processes and pathways significantly related to COVID-19 were depicted via a protein-to-protein interaction (PPI) network plotted with STRING.

2.4. Identification of hub susceptibility genes for COVID-19 in LUAD through WGCNA

WGCNA is a powerful method that facilitates the investigation of the intricate gene correlations and associations between the expression profiles of genes and phenotypes of human diseases [18]. The core principle of the WGCNA method is to transform the gene expression matrix into pairwise correlation matrices, based on which co-expressed genes in the same module can be identified [19]. In this work, correlation analysis was further conducted to analyze the relationships between gene modules and clinical traits [20]. Herein, a scale-free topology network was built for all intersected susceptibility genes expressed in 77 COVID-19 patient samples and 118 non-affected control samples from the GSE161731 dataset as the input file. The information on the positive or negative diagnosis of COVID-19 coded as bivariate was the corresponding phenotypic data. The number of genes in the minimum module was set at 15, and genes that shared high connectivities with similar expression patterns were clustered into the same co-expression modules. The 10 genes with the highest gene–trait significance ($P < 0.05$) values in the module, that is, those showing most remarkable positive correlation with the phenotype of COVID-19, were regarded as the hub susceptibility genes for COVID-19 in LUAD patients. All steps of WGCNA were performed with the WGCNA package in R software v.3.6.1.

2.5. The clinical significance of the hub susceptibility genes for COVID-19 in LUAD patients

Forest plots of SMD and the summarized receiver operating characteristics (SROC) curves were created for the 10 hub susceptibility genes for COVID-19 in LUAD patients based on the compiled expression data in all collected LUAD datasets, which was accomplished with the meta package in R software and Stata v.14.0. The protein expression levels of hub susceptibility genes in LUAD and normal lung tissues were evaluated with immunohistochemistry (IHC) images obtained from the human protein atlas (HPA) database. The prognostic value of the hub susceptibility genes for LUAD patients was assessed through Kaplan–Meier survival curves in the KM plotter database. The prognostic data used to draw the Kaplan–Meier survival curves were aggregated from 14 RNA-seq and microarray datasets, including CAARRAY, GSE14814, GSE19188, GSE29013, GSE30219, GSE31210, GSE3141, GSE31908, GSE37745, GSE43580, GSE4573, GSE50081, GSE8894, and TCGA. All LUAD patients with prognostic information on overall survival were divided into low- and high-expression groups based on the median expression value of the hub susceptibility genes. The validation of survival analyses was conducted with the Lung Cancer Explorer database for hub susceptibility genes that had significant prognostic value from the KM plotter database.

2.6. Exploration of whether there is relevance between COVID-19-related host protein expression and hub susceptibility genes

LUAD patients from the TCGA database were divided into two groups with different expression levels of hub susceptibility genes through k-means clustering methods of the NbClust package in R software v.4.1.0. The expression of TMPRSS2, a processing enzyme required for the SARS-CoV-2 infection of lung epithelia, was compared between the two groups by unpaired Students' t tests in GraphPad Prism v.8.0.1.

2.7. The effects of cigarette smoking on the expression of hub susceptibility genes in LUAD

Smoking-related effects on the expression level of 10 hub susceptibility genes were explored by comparing the differential expression of these genes in LUAD patient groups with different histories of smoking. Analysis of this part was performed using the UALCAN tool, where independent student's t-test was employed for comparison between subgroups of LUAD patients.

2.8. Correlations between hub susceptibility genes and immune cell infiltration in COVID-19 patients

The CIBERSORT method was employed to deduce the levels of 22 immune-infiltrating cells in the 77 COVID-19 samples obtained from the GSE161731 dataset. The correlations between the immune infiltration levels of 22 cells and the expression of hub susceptibility genes in 77 COVID-19 samples were calculated through Pearson's correlation tests.

2.9. In-depth analysis of the hub susceptibility genes for COVID-19 in LUAD

The molecular mechanisms of the hub genes in terms of endowing LUAD cases with susceptibility to COVID-19 were further investigated by predicting upstream miRNA and transcription factors (TF). We also estimated the interrelationships between hub susceptibility genes for COVID-19 in LUAD and the interactome sets of the A549 and Calu-3 cell lines. These analyses were enabled by the ChIP Enrichment Analysis (ChEA) and Coronascape databases.

3. Results

3.1. The susceptibility genes for COVID-19 in LUAD

A total of 114 datasets pertaining to LUAD were included to collect DEGs in 3931 LUAD and 3027 non-cancer lung samples. The PRISMA flow diagram for selecting eligible datasets is demonstrated in [Supplementary Fig. 1](#). The details of the 114 datasets and two datasets related to SARS-CoV-2 infection in LUAD cells (GSE147507 and GSE163547) are provided in [Supplementary Table 1](#). According to the filtering criteria for DEGs, 6455 up-regulated DEGs with positive SMD values and 4527 down-regulated DEGs with negative SMD values were reserved ([Supplementary Table 2](#)). The differential expression analysis results for GSE147507 and GSE163547 reported 851 up-regulated DEGs and 2036 down-regulated DEGs in SARS-CoV-2-infected LUAD samples versus non-affected LUAD samples ([Supplementary Fig. 2A and B](#); [Supplementary Table 3](#)). The intersection results for 6455 up-regulated DEGs in LUAD samples and 851 up-regulated DEGs in SARS-CoV-2-infected LUAD samples revealed 257 susceptibility genes for COVID-19 in LUAD ([Supplementary Fig. 2C](#)). Functional enrichment analyses of the 257 susceptibility genes for COVID-19 in LUAD indicated the significant assembly of them in biological processes and molecular functions, such as the cellular amino acid metabolic process, ncRNA processing, ribonucleoprotein complex biogenesis, catalytic activity acting on RNA, and methyl-CpG binding, as well as KEGG pathways, including proteasomes, the biosynthesis of amino acids, and one carbon pool by folate ([Supplementary Fig. 3](#); [Table 1](#)). The inter-activities between the component genes of biological processes and pathways related to RNA splicing, mitochondrial function, and proteasome are described vividly in the PPI network ([Supplementary Fig. 4](#)).

Table 1
Functional enrichment annotation for susceptibility genes for COVID-19 in LUAD.

Category	ID	Description	GeneRatio	pvalue	p.adjust	qvalue	Count
BP	GO:0006520	cellular amino acid metabolic process	20/225	1.7E-08	4.2E-05	3.8E-05	20
BP	GO:0034470	ncRNA processing	16/225	9.7E-07	1.1E-03	9.7E-04	16
BP	GO:0022613	ribonucleoprotein complex biogenesis	18/225	1.6E-06	1.1E-03	9.7E-04	18
BP	GO:0042254	ribosome biogenesis	13/225	1.7E-06	1.1E-03	9.7E-04	13
BP	GO:0034660	ncRNA metabolic process	20/225	2.1E-06	1.1E-03	9.7E-04	20
BP	GO:0031145	anaphase-promoting complex-dependent catabolic process	8/225	8.0E-06	3.4E-03	3.0E-03	8
BP	GO:1902036	regulation of hematopoietic stem cell differentiation	7/225	3.3E-05	1.2E-02	1.1E-02	7
BP	GO:0002479	antigen processing and presentation of exogenous peptide antigen via MHC class I, TAP-dependent	7/225	4.3E-05	1.3E-02	1.1E-02	7
BP	GO:0033209	tumor necrosis factor-mediated signaling pathway	10/225	5.1E-05	1.3E-02	1.1E-02	10
BP	GO:0061418	regulation of transcription from RNA polymerase II promoter in response to hypoxia	7/225	5.1E-05	1.3E-02	1.1E-02	7
CC	GO:0034709	methylosome	6/240	3.7E-09	1.2E-06	1.0E-06	6
CC	GO:0098798	mitochondrial protein complex	14/240	2.0E-06	3.3E-04	2.9E-04	14
CC	GO:0005687	U4 snRNP	4/240	8.2E-06	8.7E-04	7.7E-04	4
CC	GO:0005759	mitochondrial matrix	18/240	2.1E-05	1.7E-03	1.5E-03	18
CC	GO:0000793	condensed chromosome	11/240	5.5E-05	3.0E-03	2.6E-03	11
CC	GO:0034719	SMN-5m protein complex	4/240	5.5E-05	3.0E-03	2.6E-03	4
CC	GO:0046540	U4/U6 × U5 tri-snRNP complex	5/240	1.0E-04	4.2E-03	3.7E-03	5
CC	GO:0097526	spliceosomal tri-snRNP complex	5/240	1.0E-04	4.2E-03	3.7E-03	5
CC	GO:0000502	proteasome complex	6/240	1.3E-04	4.2E-03	3.7E-03	6
CC	GO:0034708	methyltransferase complex	7/240	1.4E-04	4.2E-03	3.7E-03	7
MF	GO:0140098	catalytic activity, acting on RNA	15/237	5.7E-06	2.6E-03	2.4E-03	15
MF	GO:0008327	methyl-CpG binding	4/237	1.2E-04	2.4E-02	2.2E-02	4
MF	GO:0051082	unfolded protein binding	7/237	1.6E-04	2.4E-02	2.2E-02	7
MF	GO:0016840	carbon-nitrogen lyase activity	3/237	4.1E-04	4.6E-02	4.2E-02	3
KEGG	hsa03050	Proteasome	6/117	4.7E-05	7.7E-03	7.1E-03	6
KEGG	hsa01230	Biosynthesis of amino acids	7/117	9.6E-05	7.9E-03	7.4E-03	7
KEGG	hsa00670	One carbon pool by folate	4/117	1.7E-04	9.1E-03	8.4E-03	4
KEGG	hsa05014	Amyotrophic lateral sclerosis	15/117	2.2E-04	9.1E-03	8.4E-03	15
KEGG	hsa03040	Spliceosome	9/117	3.2E-04	9.3E-03	8.6E-03	9
KEGG	hsa03013	RNA transport	10/117	3.4E-04	9.3E-03	8.6E-03	10
KEGG	hsa03008	Ribosome biogenesis in eukaryotes	7/117	1.0E-03	2.4E-02	2.2E-02	7
KEGG	hsa05022	Pathways of neurodegeneration - multiple diseases	16/117	1.2E-03	2.6E-02	2.4E-02	16

Note: BP: biological process; CC: cellular component; MF: molecular function; KEGG: Kyoto Encyclopedia of Genes and Genomes. Only top ten significant terms were displayed in the table.

3.2. Identification of hub susceptibility genes for COVID-19 in LUAD

Based on a hierarchical clustering of topological overlap matrix (TOM)-based dissimilarity and an amalgamation of modules with close relationships, the 257 susceptibility genes were merged into three modules (Fig. 1). A correlation analysis between the module Eigengenes and the trait data of COVID-19 patients and control subjects suggested that the brown module showed the most notable positive correlation with a diagnosis of COVID-19 ($r = 0.334$, $P < 0.001$; Table 2). The identification of hub susceptibility genes for COVID-19 in LUAD was restricted to the brown module, and 10 genes, MEA1, MRPL24, PPIH, EBNA1BP2, MRTO4, RABEPK, TRMT112, PFDN2, PFDN6, and NDUFS3, with the highest gene-trait significance were confirmed as the hub susceptibility genes for COVID-19 in LUAD (Table 3).

3.3. Obvious up-regulated expression and prognostic significance of hub susceptibility genes in LUAD

All 10 hub susceptibility genes for COVID-19 exhibited remarkable overexpression in LUAD samples compared to non-cancer lung samples, and the differential expression of most of the hub susceptibility genes for COVID-19 could be used to moderately discriminate LUAD from non-cancer lung samples (Supplementary Figs. 5–8). The IHC staining results further confirmed the higher expression levels of TRMT112, PFDN6, and NDUFS3 in LUAD tissues than in normal lung tissues (Supplementary Fig. 9). The up-regulation of five hub susceptibility genes, MEA1, MRPL24, PFDN2, PFDN6, and NDUFS3, served as a significant indicator of worse overall survival for LUAD patients ($P < 0.05$; Fig. 2). Among the five genes, MEA1, PFDN2, and PFDN6 were verified to exert a significant

impact on the survival of LUAD patients in the Lung Cancer Explorer database (Fig. 3).

3.4. The insignificant links between COVID-19-related host protein expression and hub susceptibility genes

LUAD patients were clustered into the k1 group (212 LUAD patients) with a low expression of 10 hub susceptibility genes and the k2 group (323 LUAD patients) with a high expression of 10 hub susceptibility genes (Fig. 4A and B). TMRSS2 expression was slightly higher in the k2 group than in the k1 group (5.163 ± 1.768 ; 5.287 ± 1.659), though without statistical significance ($P = 0.411$; Fig. 4C).

3.5. The effects of cigarette smoking on the expression of hub susceptibility genes in LUAD

Parallel expression patterns based on LUAD patients from the TCGA database indicated that smokers or reformed smokers with a history of more than 15 years exhibited higher levels of MRPL24, EBNA1BP2, PFDN2, and PFDN6 than nonsmokers ($P < 0.05$; Supplementary Fig. 10).

3.6. Correlations between hub susceptibility genes and immune cell infiltration in COVID-19 patients

The proportions of various immune cells in the 77 COVID-19 patient samples are illustrated in the composition map shown in Fig. 5. The correlation analysis of the expression of the 10 hub susceptibility genes and the infiltration levels of 23 immune cells in the COVID-19 samples reflect the fact that the fraction of plasma

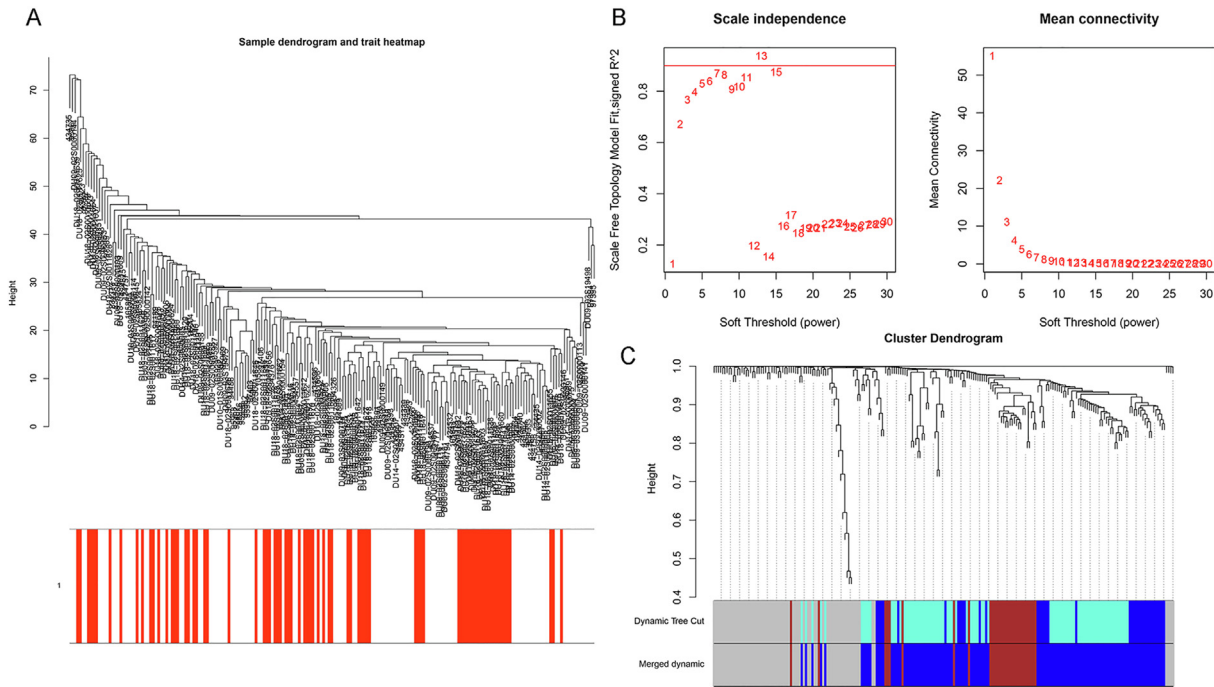


Fig. 1. Weighted gene co-expression network analysis results for susceptibility genes for COVID-19 in LUAD. A. Sample dendrogram and heatmap of the diagnostic information on COVID-19 based on the GSE161731 dataset. The name of each sample was labeled in the dendrogram. The red bar indicates the diagnosis of COVID-19. B. The selection of the best soft thresholding power. The red line represents the cut-off value of the evaluation parameters of the scale-free network ($R^2 = 0.9$). C. Cluster dendrogram and the merged gene modules. Bars in different colors distinguish different gene modules. (For interpretation of the references to color in this figure legend, the reader is referred to the web version of this article.)

Table 2
Correlations between module Eigengenes and the diagnosis of COVID-19 patients.

Module	Correlation coefficient	P value
blue	0.311591	9.25E-06
brown	0.3338057	1.85E-06
grey	-0.2565495	2.94E-04

Table 3
Genes significantly correlated with the diagnosis of COVID-19 from brown module.

Probes	Module color	Gene-trait significance	P value of gene-trait significance	Module membership	P value of module membership
MEA1	brown	0.449270087	4.46E-11	0.809177779	1.89E-46
MRPL24	brown	0.409941997	2.66E-09	0.85769273	1.17E-57
PPIH	brown	0.394952303	1.11E-08	0.863048632	3.78E-59
EBNA1BP2	brown	0.394183684	1.19E-08	0.872920332	4.55E-62
MRT04	brown	0.362115455	1.97E-07	0.81075742	9.21E-47
RABEPK	brown	0.346438643	7.01E-07	0.711785814	1.97E-31
TRMT112	brown	0.328666689	2.72E-06	0.827330611	3.14E-50
PFDN2	brown	0.318871762	5.54E-06	0.884069056	1.13E-65
PFDN6	brown	0.314612188	7.49E-06	0.848636997	2.83E-55
NDUFS3	brown	0.312333732	8.78E-06	0.882734205	3.19E-65
MRPL57	brown	0.307083049	1.26E-05	0.883942162	1.25E-65
PSMA7	brown	0.297202059	2.45E-05	0.778829158	5.89E-41
NME1	brown	0.282170279	6.43E-05	0.4790863	1.39E-12
SNRPF	brown	0.266739081	0.00016365	0.906207262	4.48E-74
GNL2	brown	0.252828898	0.000362504	0.874285624	1.72E-62
TIMM23	brown	0.246588005	0.000510675	0.815121776	1.22E-47
NDUFA6	brown	0.246509495	0.000512853	0.82519979	9.18E-50
SNRPD3	brown	0.246276027	0.000519381	0.870535107	2.43E-61
ADSL	brown	0.206493534	0.003776313	0.864879379	1.13E-59
SNRPD1	brown	0.186960302	0.008868284	0.819175371	1.77E-48
ERH	brown	0.173434462	0.015320465	0.708157272	5.40E-31
ROMO1	brown	0.165878881	0.020473293	0.581007567	5.37E-19

Note: The top ten genes were designated as the hub susceptibility genes for COVID-19 in LUAD.

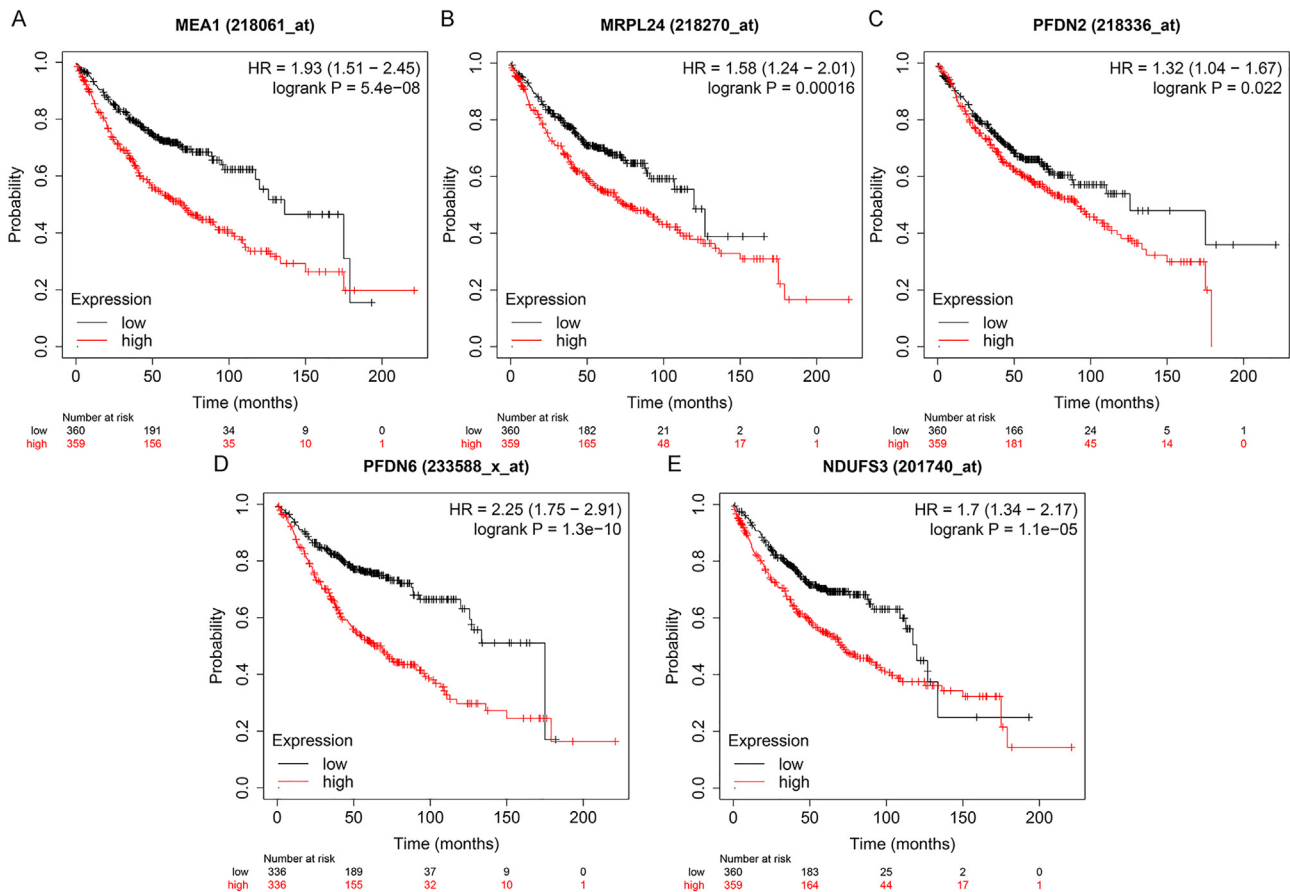


Fig. 2. Prognostic analysis results for five hub susceptibility genes in LUAD. A. Kaplan–Meier survival curves on the impact of MEA1 expression on the overall survival of LUAD patients. B. Kaplan–Meier survival curves on the impact of MRPL24 expression on the overall survival of LUAD patients. C. Kaplan–Meier survival curves on the impact of PFDN2 expression on the overall survival of LUAD patients. D. Kaplan–Meier survival curves on the impact of PFDN6 expression on the overall survival of LUAD patients. E. Kaplan–Meier survival curves on the impact of NDUFS3 expression on the overall survival of LUAD patients. HR: hazard ratio. The black and red lines delineate the overall survival probability of LUAD patients in the low and high expression groups, respectively. (For interpretation of the references to color in this figure legend, the reader is referred to the web version of this article.)

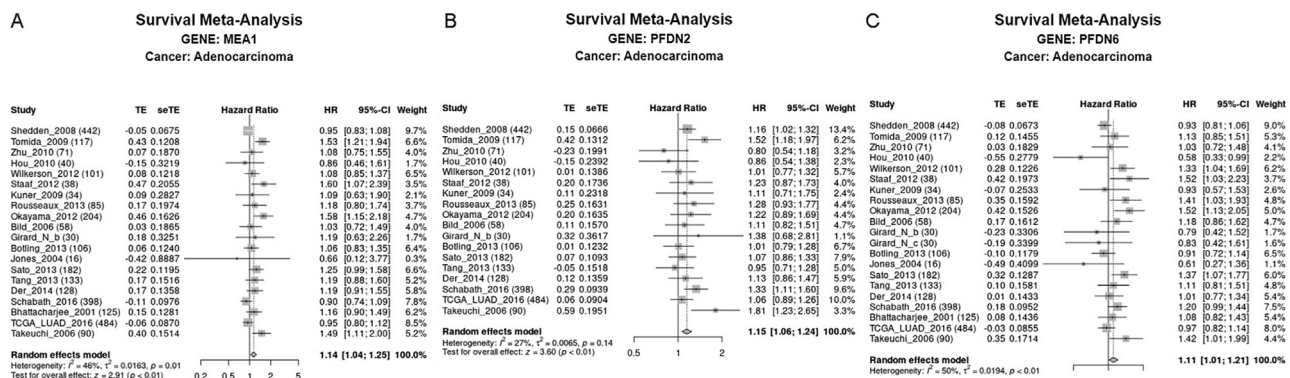


Fig. 3. The validation of the survival analysis for susceptibility genes in LUAD. A. Forest plots of the hazard ratio value for MEA1. B. Forest plots of the hazard ratio value for PFDN2. C. Forest plots of the hazard ratio value for PFDN6. TE: Estimate of treatment effect. SETE: Standard error of treatment estimate.

3.7. In-depth analysis of the hub susceptibility genes for COVID-19 in LUAD

The topological network in [Supplementary Fig. 11](#) displays upstream miRNAs or TFs that may regulate the transcription of the 10 hub susceptibility genes. Particularly, TFs, such as SP1, ELK1, and GABPA, and miRNAs, such as hsa-miR-206, hsa-miR-548a-5p, and hsa-miR-548c-5p, could target more than one hub susceptibility gene. The 10 hub susceptibility genes and eight interactome sets of the A549 cell lines exhibited overlaps at both

the gene level and the shared term level ([Fig. 7](#)); no interrelationships were found between the 10 hub susceptibility genes and the interactome sets of Calu-3 cell lines (data not shown).

4. Discussion

The COVID-19 pandemic has resulted in great challenges in the clinical management of cancer patients, especially LUAD patients [21–23]. More attention should be paid to LUAD patients with COVID-19 to improve their life conditions. Great efforts have been

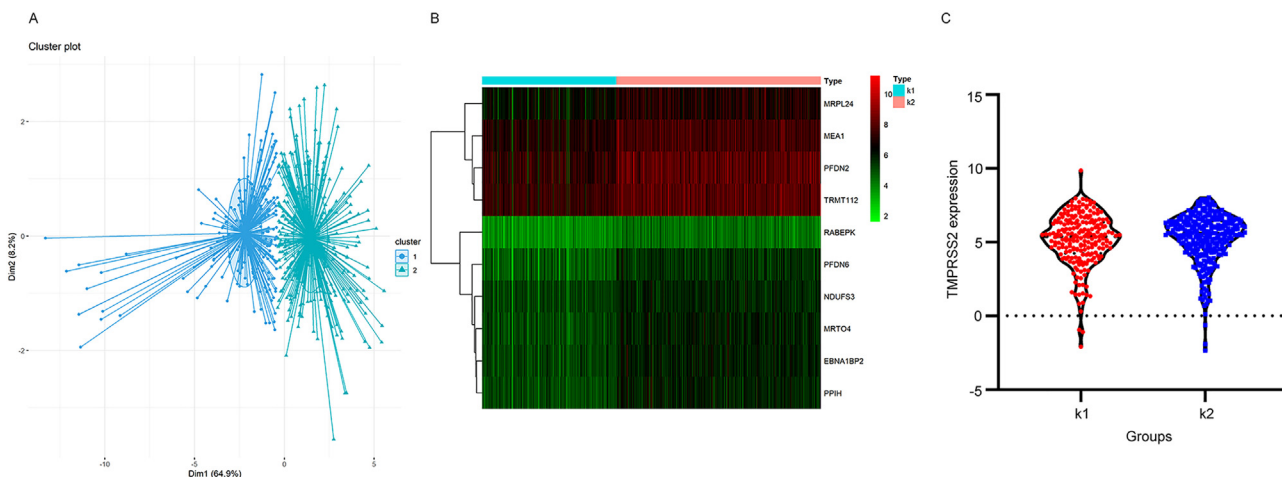


Fig. 4. K-means clustering of LUAD patients based on hub susceptibility genes and TMPRSS2 expression in different groups. A. Cluster plot. LUAD patient samples in clusters 1 or 2 are represented by blue dots and green triangles, respectively. B. Heatmap of the expression characteristics of hub susceptibility genes in two clusters of LUAD samples. C. Box plot of TMPRSS2 expression in LUAD samples of clusters 1 and 2. (For interpretation of the references to color in this figure legend, the reader is referred to the web version of this article.)

Proportions of different immune cells in 77 COVID-19 patient samples

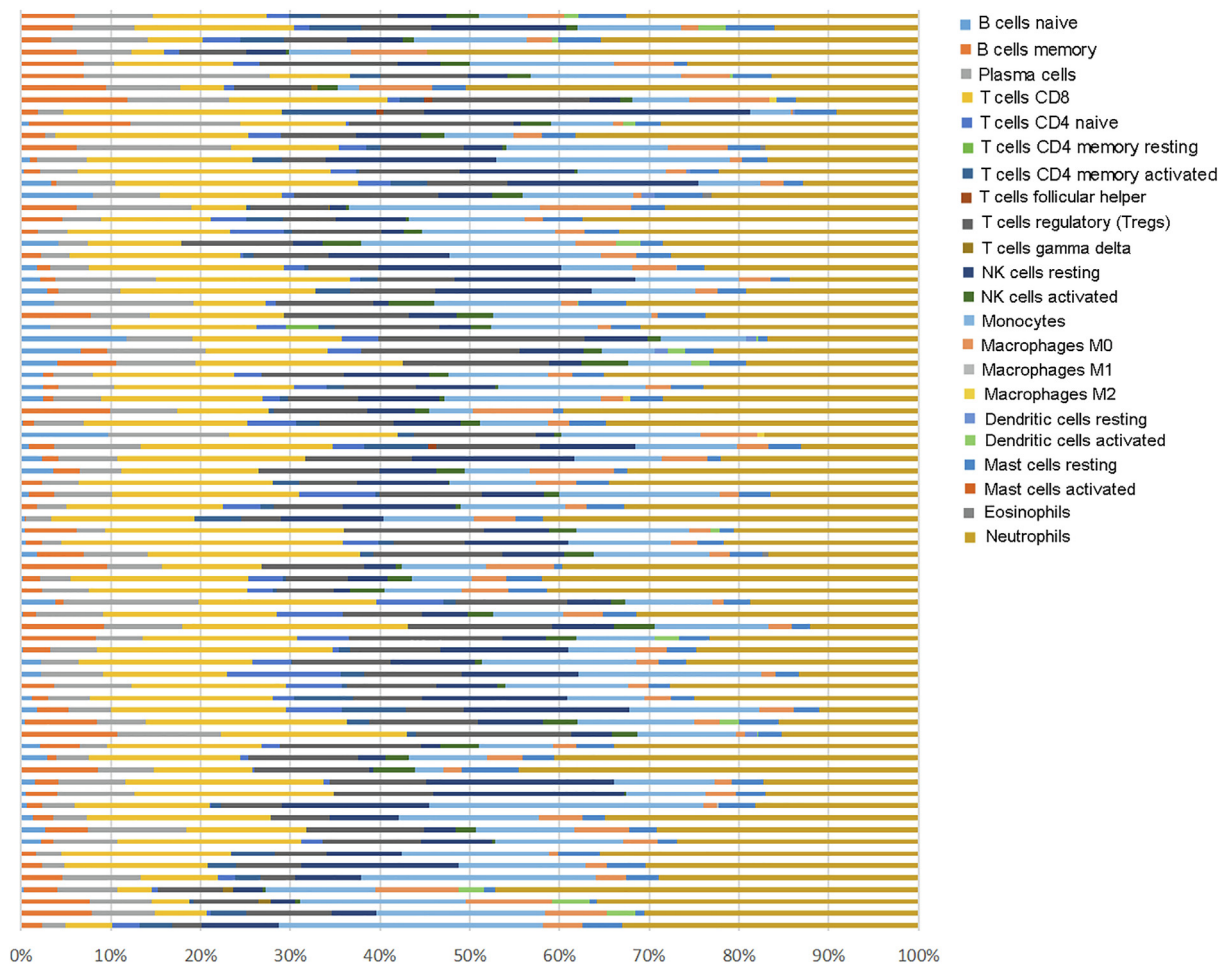


Fig. 5. The scale-stacked bar plot of the proportions of various immune cells in 77 COVID-19 patient samples. The fractions of the infiltration levels of various immune cells are represented in bars of different colors.

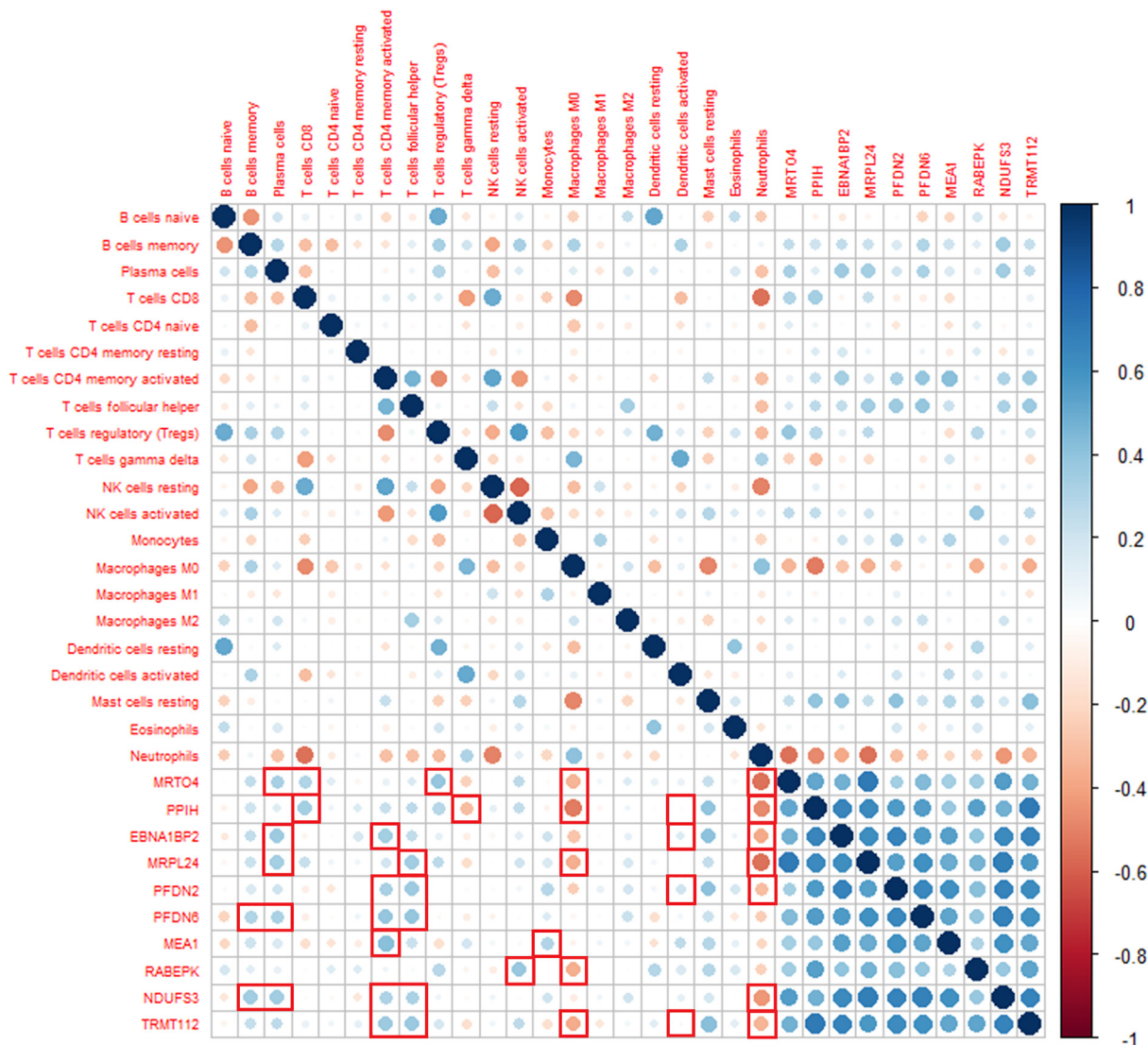


Fig. 6. The correlation diagram of the relationships between the infiltration levels of various immune cells and the expression of hub susceptibility genes in COVID-19 samples. Positive and negative correlations are indicated in blue and red colors, respectively. The size of nodes indicated the absolute value size of the correlation coefficient. Significant correlation results are marked with a red box. (For interpretation of the references to color in this figure legend, the reader is referred to the web version of this article.)

devoted by previous researchers to conquer COVID-19's impact on LUAD patients. Luo et al. carried out a bioinformatics study with multiple databases to analyze the prognostic value and mechanism of the proprotein convertase, *FURIN*, in LUAD [24]. Uddin et al. investigated the association of *ACE2* expression with immune signatures, immune ratios, and pathways in LUAD through the computational analysis of the expression profile of *ACE2* in LUAD from the TCGA and GEO databases [11]. The work of Tang et al. demonstrated the expression characteristics of *ACE2*, *TMPRSS2*, and *AAK1* in LUAD and their influence on immune infiltration via differential expression analysis, enrichment pathway analysis, and the estimation of immune cell infiltration in LUAD [25]. However, the scientific mechanism underlying the high susceptibility of LUAD patients to COVID-19 had not been clarified. We are the first group to expound on the mechanism of the high vulnerability of LUAD patients to COVID-19 through the landscape profiling of the differentially expressed genes between LUAD samples infected with SARS-CoV-2 and non-infected LUAD samples.

In the process of obtaining the susceptibility genes for COVID-19 in LUAD, unlike the traditional practice of gathering DEGs

merely from datasets of COVID-19 and uninfected samples, the susceptibility genes for COVID-19 in LUAD were gathered from 49 SARS-CoV-2-infected LUAD samples and 24 non-affected LUAD samples, as well as 3931 LUAD samples and 3027 non-cancer lung samples in globally compiled RNA-seq and microarray datasets. The narrowing of the search range to the common up-regulated DEGs in LUAD and up-regulated DEGs in SARS-CoV-2-infected LUAD samples might enhance the relevance of the identified genes to COVID-19. Functional enrichment analyses of the selected susceptibility genes implied potential biological processes, molecular functions, and pathways through which these genes may make LUAD patients more likely to develop COVID-19. We noted that several of the enriched biological process terms were associated with RNA splicing and mitochondrial functions. Previous studies on COVID-19 have provided evidence regarding the impact of COVID-19 on RNA splicing and mitochondrial functions. Singh et al. suggested that SARS-CoV-2 might cause mitochondrial dysfunctions via downregulating the ribosomal, mitochondrial complex I, and mitochondrial fission-promoting genes [26]. Banerjee et al. reported that NSP16, a non-structural protein encoded by

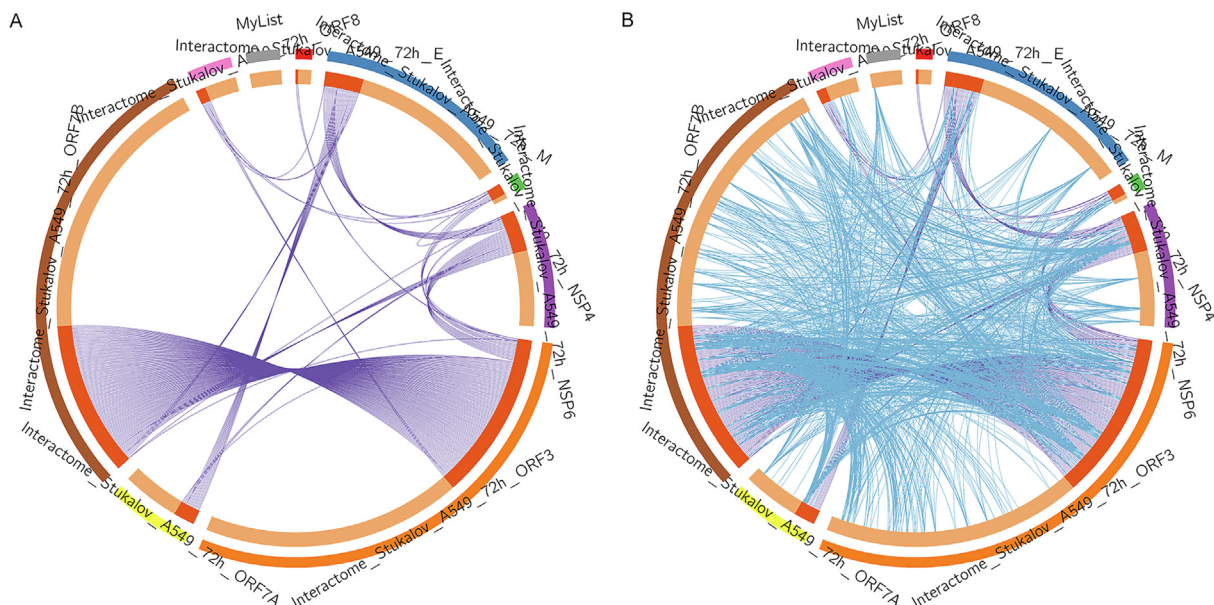


Fig. 7. Overlap between hub susceptibility genes and eight interactome sets of the A549 cell lines. A. Overlaps at the gene level, in which identical genes are linked by purple curves; B. Overlaps at the shared term level, in which genes belonging to the same ontology term are linked by blue curves. (For interpretation of the references to color in this figure legend, the reader is referred to the web version of this article.)

SARS-CoV-2, could inhibit global mRNA splicing by combining with the mRNA recognition domains of the U1 and U2 splicing of RNAs [27]. The most significant pathway was clustered near the susceptibility genes; proteasomes, which play crucial roles in viral replication processes, and proteasome inhibitors were proposed by Longhitano et al. as promising therapeutic strategies for COVID-19 [28–30]. The above functional annotation results imply that these susceptibility genes may increase LUAD patients' risk of COVID-19 by participating in the biological processes and pathways of RNA splicing, mitochondrial functions, and proteasomes.

Another fruitful finding of the current study is that several of the hub susceptibility genes, including MEA1, PFDN2, and PFDN6, were proven by both training and validation sets to be significantly related to the poor survival of LUAD patients. Many studies have reported DEGs with prominent prognostic value in LUAD; the prognostic significance of the hub susceptibility genes in LUAD from the present study is also noteworthy and might be alternatives as survival indicators of LUAD patients in future clinical practice.

There have been interesting studies pointing out that cigarette smoking exerts boosting effects on the membrane expression of genes, including ACE2, in lung epithelial cells, thus increasing the risk of contracting COVID-19 [31,32]. To determine about whether cigarette smoking also had a certain effect on the expression of the 10 hub susceptibility genes, we conducted gene expression analysis in non-smoker versus smoker groups, and we were surprised to find the higher expression of four hub susceptibility genes, including MRPL24, EBNA1BP2, PFDN2, and PFDN6, in LUAD smokers. The results imply that the increased susceptibility of LUAD smokers to COVID-19 compared to LUAD non-smokers might partly be attributed to the stimulating effects of cigarette smoking on the expression of these susceptibility genes.

It was found that innate and adaptive immune cells extensively infiltrated fatal COVID-19 lungs [33]. In respiratory epithelial cells and cardiomyocytes, SARS-CoV-2 could induce innate immune responses mediated by double-stranded RNA [34], which demonstrated the considerable immune response stimulated by SARS-CoV-2. Therefore, we also checked the correlations between the expression of susceptibility genes and the infiltration level of immune cells in COVID-19 samples. Of the 10 hub susceptibility

genes for COVID-19, PPIH was one of the host proteins engaged in the regulation of the calcineurin/NFAT pathway, thus playing a vital role in immune cell activation [35,36]. The work of Susanne et al. indicated the redundant interaction between immunophilins, including PPIH, and CoV non-structural protein 1 [37]. MRTO4 was also found to be associated with the virus-induced immune response and has been screened out as one of the key genes in human antigen-presenting cells activated by the polio vaccine [38]. The connection between TRMT112 and T cells could be traced to the study by Kohei et al., in which TRMT112 was distinctively differentially expressed between T cell subsets from paroxysmal nocturnal hemoglobinuria patients and healthy control subjects [39]. Corresponding to the findings in prior studies, the significant relationships between the 10 hub susceptibility genes and the fractions of immune cells in the current study hinted at the potential involvement of the hub susceptibility genes in the immune activities of the human body against SARS-CoV-2.

Interesting results regarding the virus–host interface have been yielded by the PPI maps of SARS-CoV-2 proteins and human proteins via AP-MS and BioID, which facilitated the recognition of the pathogenicity of SARS-CoV-2 [40–44]. Therefore, it was necessary to explore the overlaps between hub susceptibility genes for COVID-19 and the interactome sets of A549 cells in response to COVID-19. The interrelations between the hub susceptibility genes and the interactome sets of the A549 cell lines provide useful clues regarding the molecular mechanisms of these hub genes in rendering LUAD patients vulnerable to COVID-19 infection.

5. Conclusion

In summary, we identified a string of susceptibility genes for COVID-19 in LUAD. These susceptibility genes, MEA1, MRPL24, PPIH, EBNA1BP2, MRTO4, RABEPK, TRMT112, PFDN2, PFDN6, and NDUFS3, may increase the vulnerability of LUAD patients to COVID-19 by interfering with multiple biological processes and pathways, such as RNA splicing, mitochondrial functions, and the proteasome or immune functions of the human body. Further, *in vitro* and *in vivo* experiments should be carried out in future work to validate the functional roles and immunity correlations

of hub susceptibility genes in increasing the risk of COVID-19 infection in LUAD patients. Additionally, future studies could examine the antibody levels for viral antigens, particularly the anti-SPIKE antibody, after natural infection or after vaccination in LUAD samples with high or low expressions of the 10 susceptibility genes. These were also the limitations of the present work. Nevertheless, the findings in the current study may shed new light on the high susceptibility of LUAD patients to COVID-19.

Data availability

The data underlying this article are available in the article and its online supplementary material.

Declaration of Competing Interest

The authors declare that they have no known competing financial interests or personal relationships that could have appeared to influence the work reported in this paper.

Acknowledgement

This work was supported by: Guangxi Zhuang Autonomous Region Medical Health Appropriate; Technology Development and Application Promotion Project (S2020031); Guangxi Medical High-level Key Talents Training “139” Program (2020); Guangxi Medical University Training Program for Distinguished Young Scholars (2017); Medical Excellence Award Funded by the Creative Research Development Grant from the First Affiliated Hospital of Guangxi Medical University (2016); Guangxi Degree and Postgraduate Education Reform and Development Research Projects, China (JGY2019050); Guangxi Educational Science Planning Key Project (2021B167); Guangxi Higher Education Undergraduate Teaching Reform Project (2020)JA146); Guangxi Medical University Education and Teaching Reform Project (2019XJGZ04); Innovation Project of Guangxi Graduate Education (YCSW2021121). We sincerely thank for the technical support provided by Guangxi Key Laboratory of Medical Pathology.

Appendix A. Supplementary material

Supplementary data to this article can be found online at <https://doi.org/10.1016/j.csbj.2021.11.026>.

References

- Han HJ, Nwagwu C, Anyim O, Ekweremadu C, Kim S. COVID-19 and cancer: From basic mechanisms to vaccine development using nanotechnology. *Int Immunopharmacol* 2021;90:107247. <https://doi.org/10.1016/j.intimp.2020.107247>.
- Moujaess E, Kourie HR, Ghosn M. Cancer patients and research during COVID-19 pandemic: A systematic review of current evidence. *Crit Rev Oncol Hematol* 2020;150:102972. <https://doi.org/10.1016/j.critrevonc.2020.102972>.
- Chung JY, Thone MN, Kwon YJ. COVID-19 vaccines: The status and perspectives in delivery points of view. *Adv Drug Deliv Rev* 2021;170:1–25. <https://doi.org/10.1016/j.addr.2020.12.011>.
- Liu C, Zhao Y, Okwan-Duodu D, Basho R, Cui X. COVID-19 in cancer patients: risk, clinical features, and management. *Cancer Biol Med* 2020;17:519–27. <https://doi.org/10.20892/j.issn.2095-3941.2020.0289>.
- Baharoon S, Memish ZA. MERS-CoV as an emerging respiratory illness: A review of prevention methods. *Travel Med Infect Dis* 2019;32:101520. <https://doi.org/10.1016/j.tmaid.2019.101520>.
- Li Q, Guan X, Wu P, Wang X, Zhou L, Tong Y, et al. Early Transmission Dynamics in Wuhan, China, of Novel Coronavirus-Infected Pneumonia. *N Engl J Med* 2020;382(13):1199–207. <https://doi.org/10.1056/NEJMoa2001316>.
- Tan J, Yang C. Prevention and control strategies for the diagnosis and treatment of cancer patients during the COVID-19 pandemic. *Br J Cancer* 2020;123(1):5–6. <https://doi.org/10.1038/s41416-020-0854-2>.
- Guo Y-R, Cao Q-D, Hong Z-S, Tan Y-Y, Chen S-D, Jin H-J, et al. The origin, transmission and clinical therapies on coronavirus disease 2019 (COVID-19) outbreak - an update on the status. *Mil Med Res* 2020;7(1). <https://doi.org/10.1186/s40779-020-00240-0>.
- Zhou F, Yu T, Du R, Fan G, Liu Y, Liu Z, et al. Clinical course and risk factors for mortality of adult inpatients with COVID-19 in Wuhan, China: a retrospective cohort study. *Lancet* 2020;395(10229):1054–62. [https://doi.org/10.1016/S0140-6736\(20\)30566-3](https://doi.org/10.1016/S0140-6736(20)30566-3).
- Liang W, Guan W, Chen R, Wang W, Li J, Xu Ke, et al. Cancer patients in SARS-CoV-2 infection: a nationwide analysis in China. *Lancet Oncol* 2020;21(3):335–7. [https://doi.org/10.1016/S1470-2045\(20\)30096-6](https://doi.org/10.1016/S1470-2045(20)30096-6).
- Uddin MN, Akter R, Li M, Abdelrahman Z. Expression of SARS-CoV-2 cell receptor gene ACE2 is associated with immunosuppression and metabolic reprogramming in lung adenocarcinoma based on bioinformatics analyses of gene expression profiles. *Chem Biol Interact* 2021;335. <https://doi.org/10.1016/j.cbi.2021.109370>.
- Samad A, Jafar T, Rafi JH. Identification of angiotensin-converting enzyme 2 (ACE2) protein as the potential biomarker in SARS-CoV-2 infection-related lung cancer using computational analyses. *Genomics* 2020;112(6):4912–23. <https://doi.org/10.1016/j.ygeno.2020.09.002>.
- Zhang H, Quek K, Chen R, Chen J, Chen B. Expression of the SARS-CoV-2 receptor ACE2 reveals the susceptibility of COVID-19 in non-small cell lung cancer. *J Cancer* 2020;11(18):5289–92. <https://doi.org/10.7150/jca.49462>.
- Han G, Sinjab A, Hara K, Treekitkarnmongkol W, Brennan P, Chang K, et al. Single-Cell Expression Landscape of SARS-CoV-2 Receptor ACE2 and Host Proteases in Normal and Malignant Lung Tissues from Pulmonary Adenocarcinoma Patients. *Cancers (Basel)* 2021;13(6):1250. <https://doi.org/10.3390/cancers13061250>.
- Blanco-Melo D, Nilsson-Payant BE, Liu WC, Uhl S, Hoagland D, Moller R, et al. Imbalanced Host Response to SARS-CoV-2 Drives Development of COVID-19 e1039. *Cell* 2020;181:1036–45. <https://doi.org/10.1016/j.cell.2020.04.026>.
- Daamen AR, Bachali P, Owen KA, Kingsmore KM, Hubbard EL, Labonte AC, et al. Comprehensive transcriptomic analysis of COVID-19 blood, lung, and airway. *Sci Rep* 2021;11(1). <https://doi.org/10.1038/s41598-021-86002-x>.
- Ritchie ME, Phipson B, Wu D, Hu Y, Law CW, Shi W, et al. Limma powers differential expression analyses for RNA-sequencing and microarray studies. *Nucleic Acids Res* 2015;43:e47. <https://doi.org/10.1093/nar/gkv007>.
- Wan Q, Tang J, Han Y, Wang D. Co-expression modules construction by WGCNA and identify potential prognostic markers of uveal melanoma. *Exp Eye Res* 2018;166:13–20. <https://doi.org/10.1016/j.exer.2017.10.007>.
- Xu M, Ouyang T, Lv K, Ma X. Integrated WGCNA and PPI Network to Screen Hub Genes Signatures for Infantile Hemangioma. *Front Genet* 2020;11. <https://doi.org/10.3389/fgene.2020.614195614195>.
- Wu Z, Hai E, Di Z, Ma R, Shang F, Wang Y, et al. Using WGCNA (weighted gene co-expression network analysis) to identify the hub genes of skin hair follicle development in fetus stage of Inner Mongolia cashmere goat. *PLoS One* 2020;15(12):e0243507. <https://doi.org/10.1371/journal.pone.0243507>.
- Vici P, Krasniqi E, Pizzutti L, Ciliberto G, Mazzotta M, Marinelli D, et al. Burnout of health care providers during the COVID-19 pandemic: Focus on Medical Oncologists. *Int J Med Sci* 2021;18(10):2235–8. <https://doi.org/10.7150/ijms.54025>.
- Khalifeh YI, Tfayli AH. Managing Lung Cancer during Coronavirus Disease 2019 Pandemic. *Turk Thorac J* 2019;22(2021):163–8. <https://doi.org/10.5152/TurkThoracJ.2021.20110>.
- Degeling K, Baxter NN, Emery J, Jenkins MA, Franchini F, Gibbs P, et al. An inverse stage-shift model to estimate the excess mortality and health economic impact of delayed access to cancer services due to the COVID-19 pandemic. *Asia Pac J Clin Oncol* 2021. <https://doi.org/10.1111/ajco.13505>.
- Luo L, Li M, Su J, Yao X, Luo H. FURIN correlated with immune infiltration serves as a potential biomarker in SARS-CoV-2 infection-related lung adenocarcinoma. *Clin Exp Med* 2021. <https://doi.org/10.1007/s10238-021-00760-6>.
- Tang B, Zhu J, Cong Y, Yang W, Kong C, Chen W, et al. The Landscape of Coronavirus Disease 2019 (COVID-19) and Integrated Analysis SARS-CoV-2 Receptors and Potential Inhibitors in Lung Adenocarcinoma Patients. *Front Cell Dev Biol* 2020;8. <https://doi.org/10.3389/fcell.2020.577032>.
- Singh K, Chen Y-C, Hassanzadeh S, Han K, Judy JT, Seifuddin F, et al. Network Analysis and Transcriptome Profiling Identify Autophagic and Mitochondrial Dysfunctions in SARS-CoV-2 Infection. *Front Genet* 2021;12. <https://doi.org/10.3389/fgene.2021.599261>.
- Banerjee AK, Blanco MR, Bruce EA, Honson DD, Chen LM, Chow A, et al. SARS-CoV-2 Disrupts Splicing, Translation, and Protein Trafficking to Suppress Host Defenses e1321. *Cell* 2020;183:1325–39. <https://doi.org/10.1016/j.cell.2020.10.004>.
- Longhitano L, Tibullo D, Giallongo C, Lazzarino G, Tartaglia N, Galimberti S, et al. Proteasome Inhibitors as a Possible Therapy for SARS-CoV-2. *Int J Mol Sci* 2020;21(10):3622. <https://doi.org/10.3390/ijms21103622>.
- Song G, Lee EM, Pan J, Xu M, Rho H-S, Cheng Y, et al. Cheng et al., An Integrated Systems Biology Approach Identifies the Proteasome as a Critical Host Machinery for ZIKV and DENV Replication. *Genomics Proteomics Bioinform*. 2021;19(1):108–22. <https://doi.org/10.1016/j.gpb.2020.06.016>.
- Pang Y, Li M, Zhou Y, Liu W, Tao R, Zhang H, et al. The ubiquitin proteasome system is necessary for efficient proliferation of porcine reproductive and respiratory syndrome virus. *Vet Microbiol* 2021;253:108947. <https://doi.org/10.1016/j.vetmic.2020.108947>.
- Masso-Silva JA, Moshensky A, Shin J, Olay J, Nilaad S, Advani I, et al. Chronic E-Cigarette Aerosol Inhalation Alters the Immune State of the Lungs and Increases ACE2 Expression, Raising Concern for Altered Response and

- Susceptibility to SARS-CoV-2. *Front Physiol* 2021;12. <https://doi.org/10.3389/fphys.2021.649604>.
- [32] Lallai V, Manca L, Fowler CD. E-cigarette vape and lung ACE2 expression: Implications for coronavirus vulnerability. *Environ Toxicol Pharmacol* 2021;86:103656. <https://doi.org/10.1016/j.etap.2021.103656>.
- [33] Ramos da Silva S, Ju E, Meng W, Paniz Mondolfi AE, Dacic S, Green A, et al. Broad SARS-CoV-2 cell tropism and immunopathology in lung tissues from fatal COVID-19. *J Infect Dis* 2021. <https://doi.org/10.1093/infdis/jiab195>.
- [34] Li Y, Renner DM, Comar CE, Whelan JN, Reyes HM, Cardenas-Diaz FL, et al. SARS-CoV-2 induces double-stranded RNA-mediated innate immune responses in respiratory epithelial-derived cells and cardiomyocytes. *Proc Natl Acad Sci USA* 2021;118. <https://doi.org/10.1073/pnas.2022643118>.
- [35] Hogan PG, Chen L, Nardone J, Rao A. Transcriptional regulation by calcium, calcineurin, and NFAT. *Genes Dev* 2003;17(18):2205–32. <https://doi.org/10.1101/gad.1102703>.
- [36] Feske S, Giltman J, Dolmetsch R, Staudt LM, Rao A. Gene regulation mediated by calcium signals in T lymphocytes. *Nat Immunol* 2001;2(4):316–24. <https://doi.org/10.1038/86318>.
- [37] Pfefferle S, Schöpf J, Kögl M, Friedel CC, Müller MA, Carbajo-Lozoya J, et al. The SARS-coronavirus-host interactome: identification of cyclophilins as target for pan-coronavirus inhibitors. *PLoS Pathog* 2011;7(10):e1002331. <https://doi.org/10.1371/journal.ppat.1002331>.
- [38] Yanan W, Wenyong Z, Ze L, Jingxia G, Lei M, Shengjie O, et al. Identification of genes and pathways in human antigen-presenting cell subsets in response to polio vaccine by bioinformatical analysis. *J Med Virol* 2019;91(10):1729–36. <https://doi.org/10.1002/jmv.v91.1010.1002/jmv.25514>.
- [39] Hosokawa K, Kajigaya S, Keyvanfar K, Qiao W, Xie Y, Townsley DM, et al. T Cell Transcriptomes from Paroxysmal Nocturnal Hemoglobinuria Patients Reveal Novel Signaling Pathways. *J Immunol* 2017;199(2):477–88. <https://doi.org/10.4049/jimmunol.1601299>.
- [40] Terracciano R, Preianò M, Fregola A, Pelaia C, Montalcini T, Savino R. Mapping the SARS-CoV-2-Host Protein-Protein Interactome by Affinity Purification Mass Spectrometry and Proximity-Dependent Biotin Labeling: A Rational and Straightforward Route to Discover Host-Directed Anti-SARS-CoV-2 Therapeutics. *Int J Mol Sci* 2021;22(2):532. <https://doi.org/10.3390/ijms22020532>.
- [41] Gordon DE, Jang GM, Bouhaddou M, Xu J, Obernier K, White KM, et al. A SARS-CoV-2 protein interaction map reveals targets for drug repurposing. *Nature* 2020;583(7816):459–68. <https://doi.org/10.1038/s41586-020-2286-9>.
- [42] Gordon DE, Hiatt J, Bouhaddou M, Rezelj VV, Ulferts S, Braberg H, et al. Comparative host-coronavirus protein interaction networks reveal pan-viral disease mechanisms. *Science* 2020;370(6521). <https://doi.org/10.1126/science.abe9403>.
- [43] Davies JP, Almasy KM, McDonald EF, Plate L. Comparative Multiplexed Interactomics of SARS-CoV-2 and Homologous Coronavirus Nonstructural Proteins Identifies Unique and Shared Host-Cell Dependencies. *ACS Infect Dis* 2020;6:3174–89. <https://doi.org/10.1021/acsinfectdis.0c00500>.
- [44] Li J, Guo M, Tian X, Wang X, Yang X, Wu P, et al. Virus-Host Interactome and Proteomic Survey Reveal Potential Virulence Factors Influencing SARS-CoV-2 Pathogenesis. *medRxiv* 2021;2:99–112. <https://doi.org/10.1016/j.medj.2020.07.002>.